Compositional Dependence of Electrical Behaviour of Nickel-Iridium Substituted Strontium Nano-ferrites

Ekta Chaturvedi[1], **K. G. Rewatkar**[2], **V. M. Nanoti**[3].
Department of Physics,
1, Priyadarshini College of Engineering, Nagpur, India
2, Dr. Ambedkar College, Dikshabhoomi, Nagpur, India
3, Priyadarshini Institute of Engineering and Technology, Nagpur, India
E-mail – ekta.chaturvedi@gmail.com

Abstract:

The partially substituted M-type strontium ferrite ($SrFe_{12}O_{19}$) with concentration ratio of chain structure of $Sr(Ni\text{-}Ir)_xFe_{12-2x}O_{19}$ (x = 0.02 and 0.09) has been prepared using sol-gel auto combustion route by blending accompanied with fuels as urea as reducing agent. The influence of the composition on both structural and electrical properties of samples is emphasized. The powders were characterized for morphological behaviour with XRD, SEM, EDX and electrical characteristics with Impedance Analyzer. The substituted compound showed M-phase with space group $P6_3/mmc$, verified from diffraction pattern. SEM showing the formation of hexaferrite disk shape with average grain size of 22 nm - 61 nm which is further confirmed by TEM results. In this paper the variation of dielectric constant, dielectric loss, tangent loss and dc conductivity etc of the sample has been investigated. The migration of Fe^{3+} ion from octahedral site to tetrahedral site decreases the dielectric constant with increase in Ni-Ir concentration. Activation energies were calculated at both ferromagnetic and paramagnetic region. It is found that the activation energy in the paramagnetic region is higher than that in the ferromagnetic region. The enhanced resistivity of Ni-Ir substituted strontium hexaferrite is a prospective application in microwave devices.

Keywords: Sol–gel auto-combustion, magnetoplumbite, EDX, Dielectric loss, Activation Energy etc.

Introduction:

Hexagonal ferrites with magnetoplumbite (M) structure are widely used in the electronic device manufacturing industry for permanent magnets [1]. They are technologically important materials because of their unique electric, dielectric, magnetic and optical properties, which makes them suitable for many technological applications like microwave devices, transformer, electric generators, storage devices etc [2]. There is growing interest of researchers from last few decades in nanocrsytalline ferrites. The properties of these nanocrystalline ferrite particles are considerably different from those of their bulk counterparts.

The doping of Ni^{2+}-Ir^{4+} as well as preparation techniques influences the morphology and dielectric properties of this compound. The nanosized particles can be produced by a large number of methods like co precipitation, citrate precursor, sol-gel, solid state method, hydrothermal synthesis, glass crystallization, etc. This work is devoted to investigates the preparation process of Ni-Ir substituted nano hexaferrite and to show the

effect of composition on conduction, morphology and dielectric mechanism for polycrystalline $Sr(Ni\text{-}Ir)_xFe_{12-2x}O_{19}$ system prepared by improved sol-gel auto combustion technique.

2 Experimental Details:

2.1 Synthesis

The ferrites sample with composition $Sr(Ni\text{-}Ir)_xFe_{12-x}O_{19}$, (x= 0.02 and 0.09) were synthesised by using sol-gel auto combustion method also called as self propagating synthesis to study the structural and electrical properties.

2.2 Measurements:

The nanometric structure of the combusted powder and the phase composition were established by X-ray powder diffraction (Bruker Kappa Apex II D8 advance, Cu Kα radiation λ = 0.1540 nm) to determine the phase, unit cell parameters and crystalline structure. The crystalline size for each composition is calculated from XRD line width using Scherer formula

$D = k\lambda/h\cos\theta$ (1)

Where D is average size of the crystallites, k is Scherer constant (0.9), λ is wavelength of radiation (1.54056Å) and h is peak width of half height (FWHM).

The values of the lattice constants 'a', 'c' and unit cell volume 'V' were calculated by taking hkl parameters and the distance between the planes 'd', using following equation

$$\frac{1}{d_{hkl}^2} = \frac{4(h^2+hk+k^2)}{3a^2} + \frac{l^2}{c^2} \quad (2)$$

$$V = 0.866\, a^2\, c \quad (3)$$

The size and morphology of the as prepared samples were characterised by Scanning Electron Microscope (SEM, Camca SU, SEM probe) and a transmission electron microscopy (TEM-CM 200 at operating voltage of 20-200KV with the resolution of 2.4Å). The components of the ferrite were characterised by an energy dispersive spectrometer (EDS). The dielectric studies for the pelletized sample were carried out between temperatures 30°C to 350°C in the frequency range 100 Hz to 10 MHz using precision Impedance Analyzer (6500B, Waynekar electronics). The dielectric constant (ε') and dielectric loss (ε") were calculated using the following formulae

$\varepsilon' = cd/\varepsilon_o A$ (4)

$\varepsilon'' = \varepsilon' \tan\delta$ (5)

where 'c' is the capacitance, 'd; is the thickness of the sample, 'A' is the area of cross-section and 'ε_o' is the permittivity of free space.

Result and discussion:

3.1 X-ray diffraction

In this research module all the compounds were synthesised by sol-gel auto combustion method were in polycrystalline form. X-Ray diffraction pattern of developed compound of $Sr(Ni\text{-}Ir)_xFe_{12-2x}O_{19}$ (x = 0.02 and 0.09) are shown in Figure 2. XRD studies confirm the formation of hexaferrite with space group P63/mmc. The intensity diffraction peaks is found at (0 0 6), (1 0 7), (1 1 4), (2 1 3), (2 0 0) mark in figure 2. The highest intensity diffraction peak is observed at $2\theta = 33.17^0$ for the compound $Sr(Ni\text{-}Ir)_{0.02}Fe_{11.96}O_{19}$ with (1,0,7) orientation and $2\theta = 33.217$ for the sample $Sr(Ni\text{-}Ir)_{0.09}Fe_{11.82}O_{19}$ with (113) orientation. The change in relative intensities due to variation in dopant concentration of the pattern may be related to the occupation of the different crystallographic sites of the crystal lattice [4]. The decrease in crystallite size is responsible for the shift in X-ray diffraction peak towards higher diffraction angle (Table 1).

The changes in the lattice constants from a = 5.8133 Å to 5.8077 Å and c = 22.074 Å to 22.047 Å occur due to the difference between the combination of ionic radii of dopants (Ni = 0.69 Å, Ir = 0.68 Å) and the host (Fe = 0.64 Å) ions. There are five positions of Fe^{3+} in the crystal lattice of magnetoplumbite ferrite 2a , 2b , 12k , 4f1 and 4f2 , where $4f_1$ is tetrahedral site, 2b is hexahedron site and 2a, 12k and $4f_2$ are octahedral sites. The Ni^{2+} substitution of Fe^{3+} causes the shrinkage of crystal lattice, due to the volume effect for which Ni^{2+} with bigger radius must substitute Fe^{3+} in octahedral sites or probably that Ni^{2+} substitution of Fe^{3+} causes the change in the lattice binding energy. The similar trend of lattice parameter and cell volume was reported by Deepti V. Ruikar [5] in Co^{2+} substituted strontium ferrites.

The X-ray densities (ρ_{xray}) for the samples are tabulated in Table 1 which was calculated using the equation

$$\rho_{xray} = ZM/NV \qquad (6)$$

Where 'M' is the molar mass of the sample, 'N' is Avogadro's number, 'Z' is a number of molecules (Z = 2 for M-type hexaferrite) and 'V' is the volume of the cell which is calculated from equation (3). X-ray density increases with increasing Iridium and Nickel concentration which should be due to the heavier weight of Iridium and Nickel atom as compared to that of Iron atom [3][Table1]. The bulk density ρ_{bulk} values were observed to be lesser than the corresponding values of which is attributed to the generation of unavoidable pores due to composite combination during sintering process. Similar observation has been reported by Vaishali V. Soman et.al. [7].

3.2 Scanning Electron Microscope

The morphological structures of prepared compound heated at 800 °C for 4 hours are observed by scanning electron microscope, (figure 3(a) and (b)). The grains are of hexagonal-shaped platelets with particle size varies from 22.1 nm to 61.3 nm, which are further confirmed by TEM results shown in figure 4(a) and (b). The average grain size obviously tends to decrease with Ni-Ir content shown in Table 1 and figure 3 (a) and (b). It is thus reasonable to note that the Ni-Ir doping results in inhibiting grain growth [6]. As the synthesized sample possessed enough small size, hence it can be used for the application in the recording media. The chemical composition are checked by EDX which investigate the effective atomic concentration of different constituents on top surface layers of the solid shown in figure 5 (a) and (b) and table 2, the replacement of Fe^{3+} ions by Ni^{2+}-Ir^{4+} can be concluded.

3.3 Dielectric Properties

The variation of dielectric constant and dielectric loss as a function of frequency at constant temperature for Ni-Ir substituted strontium hexaferrite with different composition is shown in figure 6 (c) and (d). This behaviour is normal ferrimagnetic behaviour. The value of dielectric constant and dielectric loss rapidly decreases with increasing frequencies. Values are almost constant at higher frequencies and it is observed that the values decrease with increase in Ni^{2+} and Ir^{4+} content. Dielectric properties of the hexaferrites can be explained due to interfacial (intergranular) polarization and explained by Koops (1951) [8] on the basis of Maxwell-Wagner (1913) two layer model [9]. The decrease in dielectric constant at higher frequency can be explained on the basis that the solid is assumed as composed of well conducting grains and is separated by non conducting grain boundaries. These grain boundaries could be formed during the sintering process due to superfacial reduction or oxidation of crystallite in the porous materials as a result of their direct contact with the firing atmosphere. The high value of ε' and ε" at low frequency is due to space charge polarization produced at grain boundaries. In the polarization process exchange of electron mainly takes place between Fe^{3+} and Fe^{2+} ions for which electron have to pass from one grain to another through the poorly conducting grain boundaries which resist their flow causing accumulation of electron near the boundaries which increases the space charge polarization. At higher frequencies hopping of electron from Fe^{3+} to Fe^{2+} may not takes place so rapidly as that of the frequency of applied field and therefore change is observed [10].

3.4 Electrical Properties

The electrical conductivity of ferrites is usually described with Verwey hopping mechanism [11]. The electrical conductivity as a function of temperature of $Sr(Ni\text{-}Ir)_xFe_{12-2x}O_{19}$ hexaferrite are shown in figure 7. There is

Arrhenius behaviour in two temperature intervals with different activation energies, indicating this ferrite have semiconducting behaviour. It has been observed that electrical resistivity increases as the concentration of Ni-Ir increases. This is attributed to the fact that the substituted ions localised Fe^{2+} ions and this localization induces Verwey-de Boer hopping mechanism between Fe^{2+} and Fe^{3+} ions. The activation energy for both the sample is found to be different for ferromagnetic and paramagnetic region. The activation energy in ferromagnetic region is observed to be less than that in paramagnetic region. This is attributed to the transition from ordered (ferromagnetic) to disordered (paramagnetic) state. This resulte are in fair agreement with the observation made in case of Co-Zn ferrite by Hemeda (1994) [12].

Sample no.	Ferrite composition	Activation Energy (eV)		100KHz			ρ (MΩ-cm)
		Para	Ferro	ε‘	tanδ	ε”	
1	$Sr(Ni-Ir)_{0.02}Fe_{11.96}O_{19}$	0.48	0.03	128.667	3.856	496.223	29.54
2	$Sr(Ni-Ir)_{0.09}Fe_{11.82}O_{19}$	0.38	0.29	33.181	5.403	179.297	301.66

Table 1: Structural parameters of $Sr(Ni-Ir)_xFe_{12-2x}O_{19}$

S.no.	Composition x	Particle Size (nm)	Lattice Constant (Å)		Volume $(Å)^3$	ρ_{xray} (gm/cm^3)	ρ_{bulk} (gm/cm^3)	Porosity (%)
1	0.02	39.18	5.8133	22.074	646.01	5.47	2.92	46.48
2	0.09	21.76	5.8077	22.047	644.00	5.53	2.90	47.48

Table 2: The elements percent doped in the strontium ferrite measured by EDX.

Elements	**Atomic weight %**	
	$Sr(Ni-Ir)_{0.02}Fe_{11.96}O_{19}$	$Sr(Ni-Ir)_{0.09}Fe_{11.82}O_{19}$
Sr	2.01	6.04
Ni	0.09	0.29
Ir	0.08	0.21
Fe	32.41	32.55
O	65.41	60.91

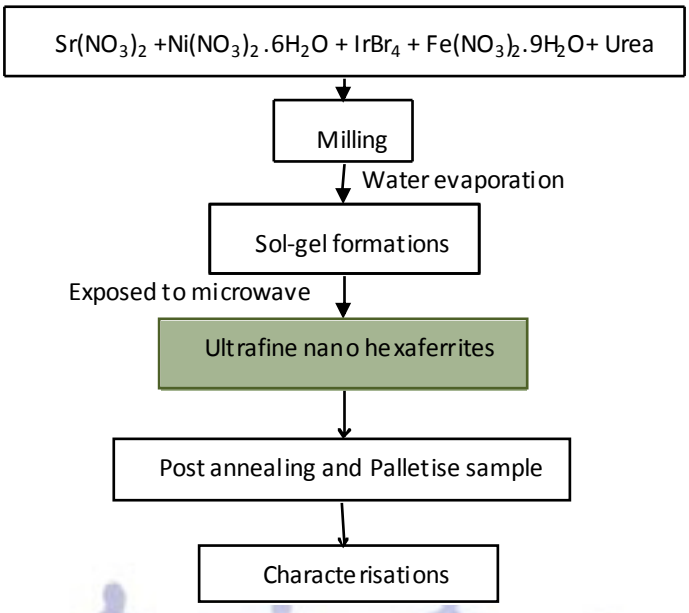

Figure 1: Flow diagram for the fabrication process of $Sr(Ni\text{-}Ir)_xFe_{12-2x}O_{19}$

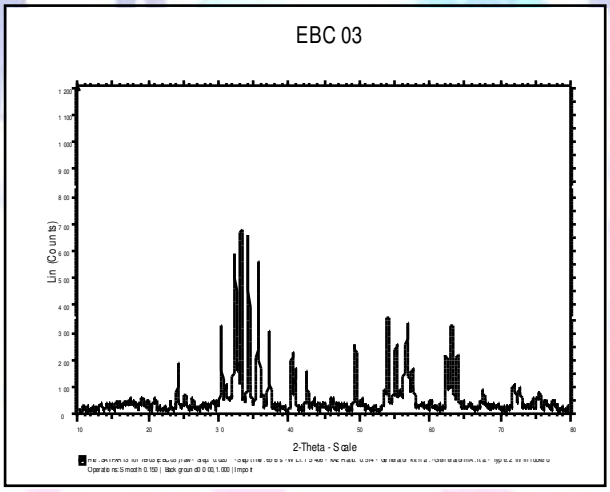

(a)

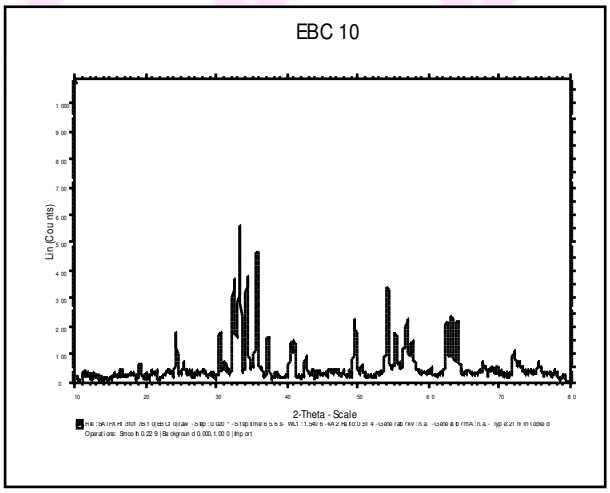

(b)

Figure. 2 : XRD spectrum of (a) $Sr(Ni\text{-}Ir)_{0.02}Fe_{11.96}O_{19}$ and (b) $Sr(Ni\text{-}Ir)_{0.09}Fe_{11.82}O_{19}$

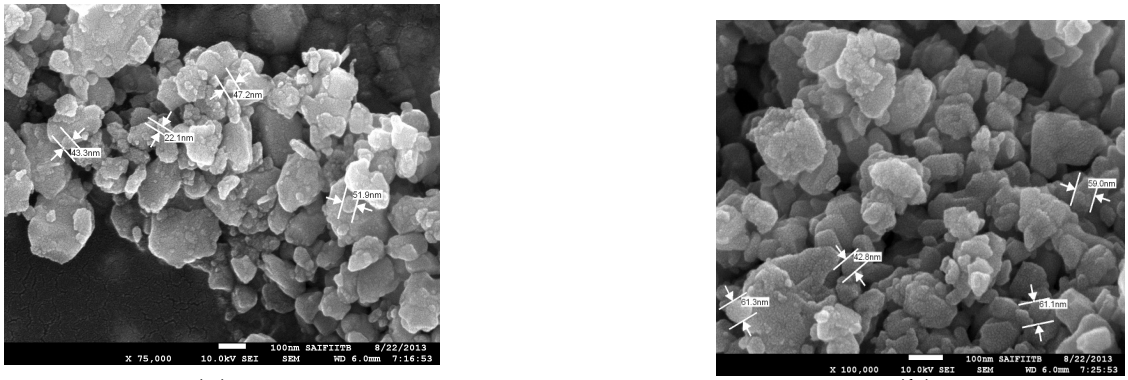

(a) (b)

Figure (3): SEM micrographs of (a) $Sr(Ni\text{-}Ir)_{0.02}Fe_{11.96}O_{19}$ (b) $Sr(Ni\text{-}Ir)_{0.09}Fe_{11.82}O_{19}$

Figure 4: TEM images of (a) $Sr(Ni\text{-}Ir)_{0.02}Fe_{11.96}O_{19}$ (b) $Sr(Ni\text{-}Ir)_{0.09}Fe_{11.82}O_{19}$

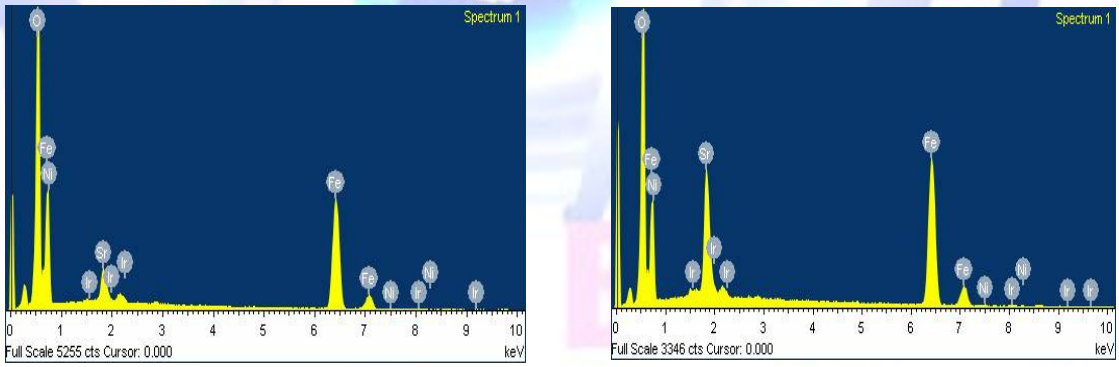

Figure 5 : EDX of (a) $Sr(Ni\text{-}Ir)_{0.02}Fe_{11.96}O_{19}$ (b) $Sr(Ni\text{-}Ir)_{0.09}Fe_{11.82}O_{19}$

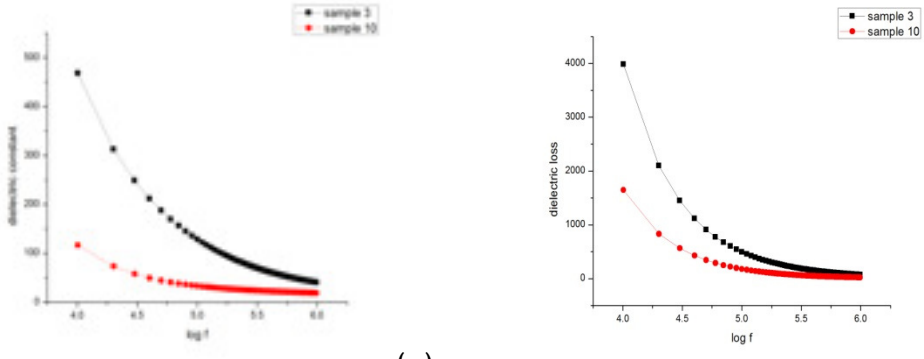

(a) (b)

Figure 6: Variation of (a) dielectric constant (b) dielectric loss

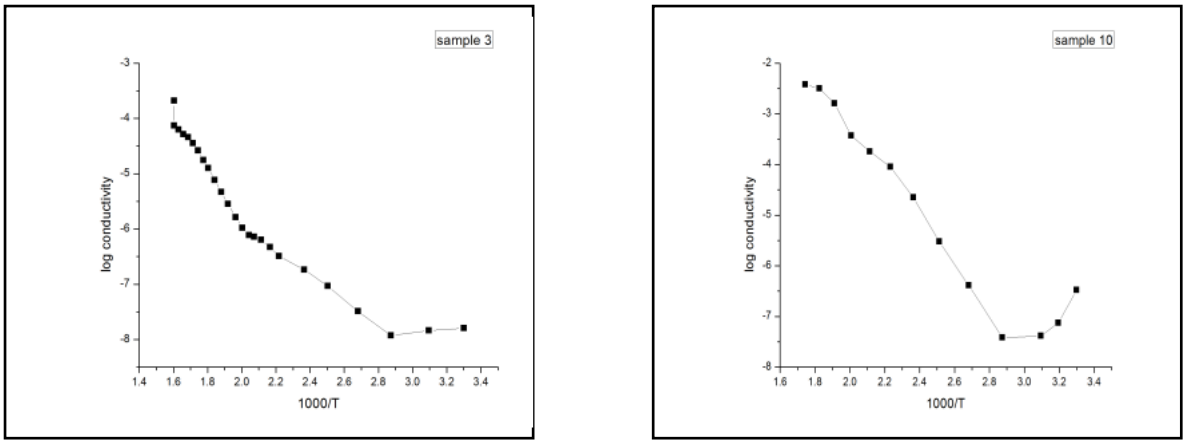

(a) (b)

Figure 7: Variation of conductivity with temperature

Conclusion:

The Ni-Ir hexaferrite nanoparticles were successfully synthesized by sol-gel auto combustion method and ferrite phase formation with space group $p6_3/mmc$ is confirmed by XRD studies. Replacement of Fe^{3+} ions has significant impact on decrease lattice parameters. The observed crystallite size in the range 22 nm to 40 nm by XRD calculation, which is in close match agreement with the TEM result with size of 22.1 nm to 61.3 nm. SEM micrographs confirmed the hexagonal structure, well formed grains with well defined grain boundaries. EDS spectra of the sample confirmed the presence of all partials of composite. The dielectric properties and structural properties of compositional dependent are well studied and found within the reported measure. The dielectric constant and dielectric loss of Ni-Ir ferrite are frequency sensitive explained by Koops model is verified in the composite at nano level. Increase in conductivity with rise in temperature shows semiconducting nature of the sample.

References:

[1] **N.Y. Lanje, D. K. Kulkarni,** Journal of magnetism and Magnetic Materials 234 (2001) 114-117.

2] **S. Gubbala, H. Nathani, K. Kaziol and R. D. K. Mishra, Physica B:** Condensed Matter 348 (2004) 317- 328.

[3] Sonal **Singhal, Tsering Namgyal, Sandeep Bansal, Kailash Chandra,** Journal of electromagnetic analysis and application 2 (2010) 376-381.

[4] **Ch. Mamatha, M. Krishnaiah, C. S. Prakash, Kishore G.Rewatkar,** Procedia Material Science 5 (2014) 780-786.

[5] **Deepti V. Ruikar, P.B. Kashid, S. Supugade, N. Pisal, Vijaya Puri,** Advances in Ceramic Science and Engineering (ACSE) 2 (2013).

[6] **S. Ounnunkad, P. Winotai,** Journal of Magnetism and Magnetic Materials 301 (2006) 292-300.

[7] **Vaishali V. Soman, V. M. Nanoti, D. K. Kulkarni, Vijay V. Soman,** Physics Procedia 54 (2014) 30-37.

[8] **C. G. Koops,** Physical review 83 (1951) 121-124.

[9] **K. W. Wagner,** Annals of Physics (Leipzig) 40 (1913) 817.

[10] **Vaishali V. Soman, V. M. Nanoti, D. K. Kulkarni,** Ceramics International 39 (2013) 5713-5723.

[11] **E. J. Verwey, P. W. Haayman and F.C. Romeijn,** Journal of chemical Physics 15 (1947) 181.

[12] **O. M. Hemeda,** Phase transition 51 (1994) 87-95.